

Bound for Gaussian-state Quantum illumination using direct photon measurement

Su-Yong Lee,^{*} Dong Hwan Kim,[†] Yonggi Jo, Taek Jeong, Duk Y. Kim, and Zaeill Kim
Agency for Defense Development, Daejeon 34186, Korea
(Dated: October 5, 2022)

We present bound for quantum illumination with Gaussian state when using on-off detector or photon number resolving detector, where its performance is evaluated with signal-to-noise ratio. First, in the case of coincidence counting, the best performance is given by two-mode squeezed vacuum (TMSV) state which outperforms coherent state and classically correlated thermal (CCT) state. However coherent state can beat the TMSV state with increasing signal mean photon number when using the on-off detector. Second, the performance is enhanced by taking Fisher information approach of all counting probabilities including non-detection events. In the Fisher information approach, the TMSV state still presents the best performance but the CCT state can beat the TMSV state with increasing signal mean photon number when using the on-off detector. We also show that displaced squeezed state exhibits the best performance in the single-mode Gaussian state.

Introduction. — Entanglement is indispensable for quantum teleportation, quantum sensing, and quantum illumination (QI). Contrary to the other protocols, QI loses entanglement but takes quantum advantage by survival of quantum correlation. The objective of QI is to discriminate the presence or absence of a low-reflectivity target [1, 2]. According to the frequency range of the probe signal used for QI, photon loss is the dominant limiting factor for the performance under optical wave range or thermal noise is the dominant one under microwave range. In a laboratory, a low-reflectivity beam splitter plays the role of the target and thermal noise is intentionally injected into the low-reflectivity beam splitter. Thermal noise is replaced by thermal state which is produced by scattering coherent state light with a rotating glass disk or blocking one mode of a two-mode squeezed vacuum (TMSV) state. We consider a scenario where a signal mode of an input state interacts with a target having a low reflectivity in heavy thermal noise environment, and then the reflected signal mode is measured in a receiver. If there is an idler mode of the input state, it is best to measure the idler mode with the reflected signal mode.

The performance of QI can be evaluated by quantum Chernoff bound (QCB) [3–5], which is the upper limit of lower bound on a target-detection error probability. As an input for QI, it is feasible to prepare Gaussian states, such as coherent, thermal, squeezed, and TMSV states. Among single-mode Gaussian states, coherent state presents the best performance by QCB while a displaced squeezed (DS) state is a general pure state. Among two-mode Gaussian states, TMSV state is a nearly optimal state [6, 7]. A classically correlated thermal (CCT) state, which is produced by impinging a thermal state into a beam splitter, cannot outperform the TMSV state and the coherent state by QCB.

It is important to know if it is possible to achieve the QCB with any measurement setup. Up to now, there are several measurement schemes proposed or implemented for TMSV state, CCT state, and coherent state, such

as CCD camera [8, 9], 3D camera [10], photon number difference measurement [11–13], homodyne (or heterodyne) detection [13–18], nonlinear interaction measurement [19–21], collective measurements [22], and on-off detection scheme [23] which produces signal mode conditionally by the detection of the idler mode. The QCB is asymptotically achieved with homodyne detection for coherent state [24], photon number difference measurement for CCT state [13], and sum frequency generation with feedforward for TMSV state [22].

In this paper, we consider the most feasible measurements for Gaussian-state quantum-illumination, using on-off detector and photon number resolving (PNR) detector. By measuring directly the idler and the reflected signal, we evaluate the performance bound with signal-to-noise ratio (SNR). Although the direct detection cannot take quantum advantage over the classical limit given by coherent state, we claim that TMSV state can take quantum advantage over the coherent or CCT state in the case of using the on-off detector or PNR detector. The performance is shown by coincidence counting events, and then it is enhanced by Fisher information approach using all possible counting events.

Single- and two-mode Gaussian states. — A Gaussian state is described with covariance matrix and first-order moments. The covariance matrix is described with $\sigma_{ij} = \langle \hat{R}_i \hat{R}_j + \hat{R}_j \hat{R}_i \rangle - 2\langle \hat{R}_i \rangle \langle \hat{R}_j \rangle$, where $\hat{R}_i = \hat{X}_i(\hat{P}_i)$ and $\hat{a}_k = \frac{1}{\sqrt{2}}(\hat{X}_k + i\hat{P}_k)$. The first-order moments are described with displacement, $\mu^T = \sqrt{2}(\text{Re}(\alpha), \text{Im}(\alpha))$.

A single-mode pure Gaussian state is represented by a DS state $\hat{D}(\alpha)|\xi\rangle$, where $\alpha = |\alpha|e^{i\phi}$ and $\xi = re^{i\varphi}$. After interacting the input signal with a target having reflectivity κ in thermal noise environment, the reflected output state is given by

$$\sigma_{\text{DS}}(\kappa) = \begin{pmatrix} A_1 - A_2 \cos \varphi & -A_2 \sin \varphi \\ -A_2 \sin \varphi & A_1 + A_2 \cos \varphi \end{pmatrix}, \quad (1)$$

$$\mu = \sqrt{2\kappa}|\alpha| \begin{pmatrix} \cos \phi \\ \sin \phi \end{pmatrix},$$

where $A_1 = 1 + 2N_B + 2\kappa N_{sq}$, $A_2 = 2\kappa\sqrt{N_{sq}(N_{sq} + 1)}$, $N_{sq} = \sinh^2 r$, and N_B is the mean photon number of thermal noise observed at a detector. When the target is off, the covariance matrix is $\sigma_{DS}(0)$ and the first-order moments are zero.

With no first-order moment, two-mode Gaussian states can be represented by a two-mode squeezed vacuum (TMSV) state and a classically correlated thermal (CCT) state. The former is a representative of continuous variable entangled states, and the latter is a kind of classical correlated states. After the signal mode of the TMSV state interacts with a target, the output is given by

$$\sigma_{TMSV}(\kappa) = \begin{pmatrix} B & 0 & C & 0 \\ 0 & B & 0 & -C \\ C & 0 & 1 + 2N_S & 0 \\ 0 & -C & 0 & 1 + 2N_S \end{pmatrix}, \quad (2)$$

where $B = 1 + 2N_B + 2\kappa N_S$, and $C = 2\sqrt{\kappa N_S(N_S + 1)}$. When the target is off, the covariance matrix is $\sigma_{TMSV}(0)$. After the signal mode of the CCT state interacts with the target, the output state is given by

$$\sigma_{CCT}(\kappa) = \begin{pmatrix} B & 0 & D & 0 \\ 0 & B & 0 & D \\ D & 0 & 1 + 2N_I & 0 \\ 0 & D & 0 & 1 + 2N_I \end{pmatrix}, \quad (3)$$

where $D = 2\sqrt{\kappa N_S N_I}$ and N_I is the mean photon number of the idler mode. When the target is off, the covariance is $\sigma_{CCT}(0)$.

Signal-to-Noise Ratio with coincidence counting. — The performance of discriminating the presence or absence of a target can be evaluated with a detection error probability that is represented by a sum of miss-detection probability $P(\text{off}|\text{on})$ and false-alarm probability $P(\text{on}|\text{off})$, which is minimized under the decision threshold. For equal prior probabilities, the detection error probability is given by $P_{\text{err}}^{(M)} = \frac{1}{2}[P(\text{off}|\text{on}) + P(\text{on}|\text{off})]$ whose minimum is approximately upper bounded as $P_{\text{err}}^{(M)} \approx \exp[-\text{SNR}^{(M)}]$ when the two states of target present or absent are close to each other [13, 19]. Under mode-by-mode measurements, the signal-to-noise ratio (SNR) is explicitly described with

$$\text{SNR}^{(M)} = \frac{M(\langle \hat{O} \rangle_{\kappa} - \langle \hat{O} \rangle_{\kappa=0})^2}{2[\sqrt{\Delta^2 \hat{O}_{\kappa}} + \sqrt{\Delta^2 \hat{O}_{\kappa=0}}]^2}, \quad (4)$$

where M is the number of modes, $\langle \hat{O} \rangle_{\kappa}$ is the mean value of an observable, and $\Delta^2 \hat{O}_{\kappa}$ is its variance. Increasing the SNR corresponds to decreasing the detection error probability.

On-off detection. — An observable that describes coincident on-off detection is given by $\hat{O}_{\text{on}} \equiv \bigotimes_{i=S,I} (\hat{I}_i -$

$|0\rangle_i \langle 0|)$ for signal and idler modes, where \hat{I}_i is the identity operator of mode i . With no idler mode, it only takes the signal-mode observable. Since the variance of the observable is given as $\Delta^2 \hat{O}_{\text{on}} = \langle \hat{O}_{\text{on}} \rangle (1 - \langle \hat{O}_{\text{on}} \rangle)$, the SNR of Eq. (4) is represented only with $\langle \hat{O}_{\text{on}} \rangle$.

For a single-mode Gaussian state, the mean value of the observable is obtained as $\langle \hat{O}_{\text{on}} \rangle = 1 - \text{tr}(\rho_{\text{out}}|0\rangle_S \langle 0|)$. Given a DS state, the vacuum probability from the Eq. (1) is derived as

$$\langle 0 | \rho_{\text{out}} | 0 \rangle = \frac{\exp[-\frac{\kappa|\alpha|^2}{2L}(A_1 + 1 + A_2 \cos(\varphi - 2\phi))]}{\sqrt{L}}, \quad (5)$$

where $L = (N_B + 1)^2 + \kappa N_{sq}(2 + 2N_B - \kappa)$. Then, the SNR is maximized at $\cos(\varphi - 2\phi) = 1$. At $\kappa = 0.01$ and $N_B = 600$, the SNR is maximized with $|\alpha|^2 \approx 0.918$ in the constraint of $N_S \equiv |\alpha|^2 + N_{sq} = 1$, where the DS state presents sub-Poissonian statistics. Since there is a very small difference between the SNRs of the coherent state and the DS state, we choose the coherent state as the representative of the single-mode Gaussian state in the on-off detection scheme. In the limit of N_S , $\kappa \ll 1 \ll N_B$, the SNR is approximated as $\frac{M\kappa^2 N_S^2}{8N_B^3}$.

For a two-mode Gaussian state, the mean value of the observable is obtained as $\langle \hat{O}_{\text{on}} \rangle = 1 - \text{tr}(\rho_{\text{out}}|0\rangle_S \langle 0|) - \text{tr}(\rho_{\text{out}}|0\rangle_I \langle 0|) + \text{tr}(\rho_{\text{out}}|00\rangle_{SI} \langle 00|)$. Given a TMSV state, the mean value of the observable is derived as

$$\langle \hat{O}_{\text{on}} \rangle = 1 - \frac{1}{1 + N_B + \kappa N_S} - \frac{1}{1 + N_S} + \frac{1}{(1 + N_S)(1 + N_B)}. \quad (6)$$

In the limit of N_S , $\kappa \ll 1 \ll N_B$, the SNR is approximated as $\frac{M\kappa^2 N_S}{8N_B^3}$. Given a CCT state, the mean value of the observable is derived as

$$\langle \hat{O}_{\text{on}} \rangle = 1 - \frac{1}{1 + N_B + \kappa N_S} - \frac{1}{1 + N_I} + \frac{1}{(1 + N_I)(1 + N_B) + \kappa N_S}. \quad (7)$$

In the limit of $N_S, N_I, \kappa \ll 1 \ll N_B$, the SNR is approximated as $\frac{M\kappa^2 N_S^2 N_I}{2N_B^4}$.

Fig.1(a) shows the SNRs of the three Gaussian states as a function of N_S under coincidence counting measurements using on-off detectors. The TMSV state outperforms the coherent state and the CCT state at $N_S < 0.0016$, but the coherent state presents the best performance at $N_S > 0.0016$. The CCT state can beat the TMSV state with increasing the mean photon number of the idler mode N_I , and then it can approach the coherent state performance around $N_I = 10^6$. In Fig.1(b), we show that the SNR ratio between the coherent state and the CCT state with $N_I = 10^6$ is equal to one, regardless of N_S . With deceasing N_S , it is also shown that the TMSV state can take quantum advantage over the coherent state more than five times.

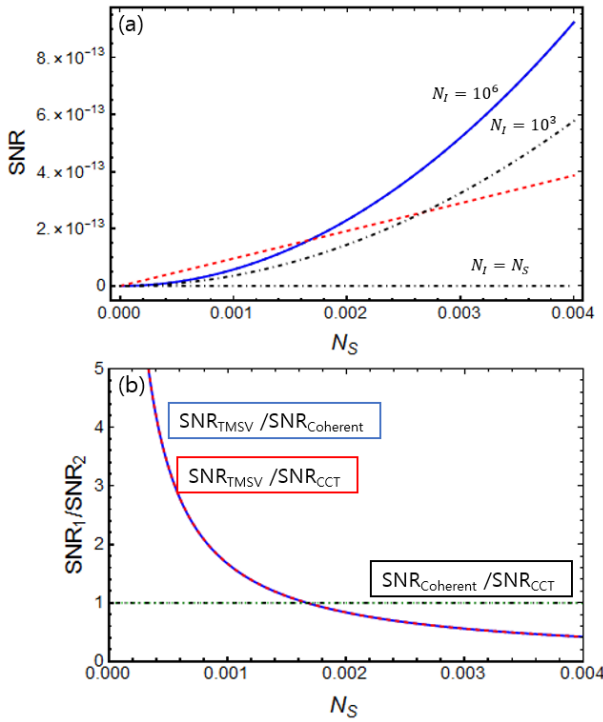


FIG. 1. Signal-to-noise ratio as a function of N_S at $\kappa = 0.01$, $N_B = 600$, $M = 10^6$, under coincidence counting measurements using on-off detectors. (a) TMSV state (red, dashed), Coherent state (blue, solid), and CCT state (black, dot-dashed). According to the mean photon number of the idler mode (N_I) in the CCT state, the CCT state can beat the TMSV state and approach the coherent state at $N_I = 10^6$. (b) Ratio of different SNRs for TMSV/Coherent (blue, solid), TMSV/CCT (red, dashed), and Coherent/CCT (black, dot-dashed) at $N_I = 10^6$. Blue and red curves are overlapped. Green dotted line indicates 1.

Photon Number Resolving detection. – An observable of coincident PNR detection is given by $\hat{n}_{SI} \equiv \bigotimes_{i=S,I} \hat{a}_i^\dagger \hat{a}_i$. It only takes the signal mode observable for a single-mode state.

For a single-mode Gaussian state, the mean value of the observable is obtained as $\langle \hat{n}_{SI} \rangle = \kappa \langle \hat{n}_S \rangle_{\text{in}} + N_B$, where subscript ‘in’ represents the input mode. Its variance is given by $\Delta^2 n_{SI} = \kappa^2 (\langle (\hat{n}_S \hat{n}_I)^2 \rangle_{\text{in}} - \langle \hat{n}_S \hat{n}_I \rangle_{\text{in}}^2) + N_B \langle \hat{n}_I^2 \rangle_{\text{in}}$, where $Q_M = \frac{\langle \hat{n}_S^2 \rangle_{\text{in}} - \langle \hat{n}_S \rangle_{\text{in}}^2}{\langle \hat{n}_S \rangle_{\text{in}}} - 1$ is the Mandel Q-factor. The SNR of Eq. (4) increases with decreasing Q_M . Thus, it is best to inject a single-mode Gaussian state having sub-Poissonian statistics, i.e., DS state, into the target. In the range of $\kappa \ll 1$, however, it is negligible to consider the sub-Poissonian contribution by a factor of κ^2 , such that it is much more feasible to prepare the coherent state than the DS state. In the limit of N_S , $\kappa \ll 1 \ll N_B$, the SNR is approximated as $\frac{M\kappa^2 N_S^2}{8N_B^2}$.

For a two-mode Gaussian state, the mean value of the observable is obtained as $\langle \hat{n}_{SI} \rangle = \kappa \langle \hat{n}_S \hat{n}_I \rangle_{\text{in}} + N_B \langle \hat{n}_I \rangle_{\text{in}}$.

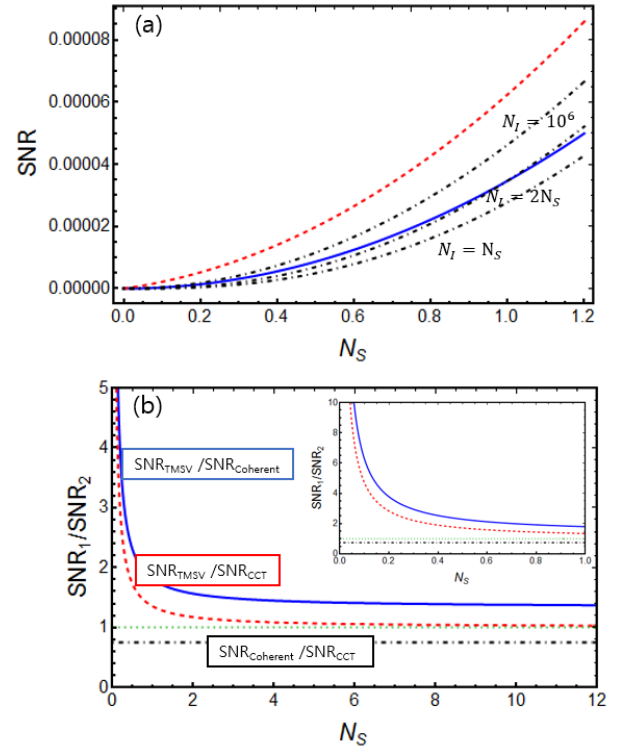


FIG. 2. Signal-to-noise ratio as a function of N_S at $\kappa = 0.01$, $N_B = 600$, $M = 10^6$, under coincidence counting measurements using PNR detectors. (a) TMSV state (red, dashed), Coherent state (blue, solid), and CCT state (black, dot-dashed). According to the mean photon number of the idler mode (N_I) in the CCT state, the CCT state can beat the coherent state. (b) Ratio of different SNRs for TMSV/Coherent (blue, solid), TMSV/CCT (red, dashed), and Coherent/CCT (black, dot-dashed) at $N_I = 10^6$. Green dotted line indicates 1.

Its variance is given by

$$\begin{aligned} \Delta^2 n_{SI} &= \kappa^2 (\langle (\hat{n}_S \hat{n}_I)^2 \rangle_{\text{in}} - \langle \hat{n}_S \hat{n}_I \rangle_{\text{in}}^2) + N_B \langle \hat{n}_I^2 \rangle_{\text{in}} \quad (8) \\ &+ N_B^2 (2 \langle \hat{n}_I^2 \rangle_{\text{in}} - \langle \hat{n}_I \rangle_{\text{in}}^2) - 2\kappa N_B \langle \hat{n}_S \hat{n}_I \rangle_{\text{in}} \langle \hat{n}_I \rangle_{\text{in}} \\ &+ \kappa (1 - \kappa + 4N_B) \langle \hat{n}_S \hat{n}_I^2 \rangle_{\text{in}}. \end{aligned}$$

In the limit of N_S , N_I , $\kappa \ll 1 \ll N_B$, the SNR of Eq. (4) is approximated as

$$\text{SNR}^{(M)} \approx \frac{M\kappa^2 \langle \hat{n}_S \hat{n}_I \rangle_{\text{in}}^2}{8[N_B^2 (2 \langle \hat{n}_I^2 \rangle_{\text{in}} - \langle \hat{n}_I \rangle_{\text{in}}^2) + N_B \langle \hat{n}_I^2 \rangle_{\text{in}}]}. \quad (9)$$

Given a TMSV state and a CCT state, the SNRs are approximated as $\frac{M\kappa^2 N_S}{16N_B^2}$ and $\frac{M\kappa^2 N_S^2 N_I}{4N_B^3}$, respectively.

Fig.2(a) shows the SNRs of the three Gaussian states as a function of N_S under coincidence counting measurements using PNR detectors. The TMSV state outperforms the other states in the whole range of N_S . With increasing N_I , the CCT state can beat the coherent state at $N_I = 2N_S$ but it cannot beat the TMSV state. In Fig.2(b), we show that the SNR ratio between the coherent state and the CCT state with $N_I = 10^6$ is less

than one, regardless of N_S . With deceasing N_S , it is also shown that the TMSV state can take quantum advantage over the coherent (or CCT) state more than ten times.

Signal-to-Noise Ratio with Fisher information approach. – In the limit of $\kappa \ll 1$, the SNR of Eq. (4) can be approximated as quantum Fisher information (QFI) [12, 25, 26] that is achieved with optimal observable. Since on-off (or PNR) detection performs measurements with orthogonal basis, the QFI is lower bounded by Fisher information (FI) that is described with the conditional probability P_n . Thus, the SNR is derived as

$$\text{SNR}^{(M)} \approx \frac{M\kappa^2}{8} H(\kappa) \geq \frac{M\kappa^2}{8} \sum_n \left. \frac{[\partial_\kappa P_n]^2}{P_n} \right|_{\kappa=0}, \quad (10)$$

where ∂_κ represents the partial derivative with respect to κ , $H(\kappa)$ is the QFI, and the function of P_n on the right-hand side is the FI. Here we consider FI using both coincidence counting probabilities and non-coincidence counting probabilities in the whole measurement process.

On-off detection. – FI using on-off detection is represented by $\sum_{i,j=\text{on, off}} \frac{[\partial_\kappa P(i,j|\kappa)]^2}{P(i,j|\kappa)}|_{\kappa=0}$. For a DS state, using Eq. (5), the SNR is approximated by $\frac{M\kappa^2 N_S^2}{8N_B(N_B+1)^2}$. For a TMSV state, using Eq. (6), the SNR is approximated by $\frac{M\kappa^2 N_S(N_S+1)}{8N_B(N_B+1)^2}$. For a CCT state, using Eq. (7), the SNR is approximated by $\frac{M\kappa^2 N_S^2}{8N_B(N_B+1)^2} [1 + \frac{N_I}{(1+N_I)^2}]$ which is maximized at $N_I = 1$. The TMSV state outperforms the other states in the range of $N_S < 4$, but the CCT state presents the best performance at $N_S > 4$.

Photon Number Resolving detection. – FI using PNR detection is represented by $\sum_{n,m} \frac{[\partial_\kappa P(n,m|\kappa)]^2}{P(n,m|\kappa)}|_{\kappa=0}$, where $P(n,m|\kappa) = \langle n, m | \rho_{\text{out}}(\kappa) | n, m \rangle_{SI}$. The probability $P(n,m|\kappa)$ can be calculated by using the Bargmann representation [27]. For the DS state, the SNR is approximated by $\frac{M\kappa^2 N_S^2}{8N_B(N_B+1)}$. For the TMSV state, the SNR is approximated by $\frac{M\kappa^2 N_S(1+2N_S)}{8N_B(N_B+1)}$. For the CCT state, the SNR is approximated by $\frac{M\kappa^2 N_S^2(1+2N_I)}{8N_B(N_B+1)(1+N_I)}$ which is maximized at $N_I \rightarrow \infty$. The TMSV state presents the best performance in the whole range of N_S . Note that the DS state cannot beat the other states in both on-off detection and PNR detection.

In Table I, we compare the SNRs that are derived from coincidence counting as well as FI at the limit of $N_S, N_I, \kappa \ll 1 \ll N_B$. Since on-off detection and PNR detection measure the diagonal components of the output states, the scaling of the SNRs is proportional to κ^2 . For each state, the PNR detection presents better performance than the on-off detection, and FI approach outperforms the coincidence counting approach. Since non-coincidence counting events also include target information, it is utilized to enhance the SNR by the FI approach. DS state presents the same ordering of SNRs between the FI and coincidence counting approaches. The

TABLE I. SNR at $N_S, N_I, \kappa \ll 1 \ll N_B$. The difference between SNRs of a displaced squeezed state and a coherent state is negligible. CC represents coincidence counting.

Input state SNR using	DS state	CCT state	TMSV state
CC (on-off detection)	$\frac{M\kappa^2 N_S^2}{8N_B^3}$	$\frac{M\kappa^2 N_S^2 N_I}{2N_B^4}$	$\frac{M\kappa^2 N_S}{8N_B^4}$
FI (on-off detection)	$\frac{M\kappa^2 N_S^2}{8N_B^3}$	$\frac{M\kappa^2 N_S^2}{8N_B^3}$	$\frac{M\kappa^2 N_S}{8N_B^3}$
CC (PNR detection)	$\frac{M\kappa^2 N_S^2}{8N_B^2}$	$\frac{M\kappa^2 N_S^2 N_I}{4N_B^2}$	$\frac{M\kappa^2 N_S}{16N_B^2}$
FI (PNR detection)	$\frac{M\kappa^2 N_S^2}{8N_B^2}$	$\frac{M\kappa^2 N_S^2}{8N_B^2}$	$\frac{M\kappa^2 N_S}{8N_B^2}$

FI approach enhances the SNR of the CCT as much as $N_B/4N_I$ times for the on-off detection and $1/2N_I$ times for the PNR detection. It also enhances the SNR of the TMSV as much as N_B times for the on-off detection and twice for the PNR detection.

Conclusion. – We have investigated the performance bound of Gaussian-state quantum-illumination using on-off detector or PNR detector, without any additional operation on the idler and the reflected signal. Under coincidence counting events, we showed that TMSV state presents the best performance, whereas coherent state can beat the TMSV state with increasing N_S when using on-off detector. Moreover, we presented that the performance of the TMSV state can be enhanced by taking FI approach of all counting probabilities including non-detection events, whereas CCT state can beat the TMSV state with increasing N_S when using on-off detector. We also found that DS state exhibits the best performance in the single-mode Gaussian state even if the advantage is very small compared to the coherent state.

On the contrary to $N_B \gg 1$, it is also interesting to consider the case of $N_B \ll 1$. When the thermal noise gets close to zero under the above results, coherent state outperforms TMSV state with increasing N_S in the cases of using both on-off and PNR detectors. At $N_B = 0$, the coherent states always presents the best performance in both cases.

This work was supported by a grant to Defense-Specialized Project funded by Defense Acquisition Program Administration and Agency for Defense Development.

* suyong2@add.re.kr

† kiow639@add.re.kr

[1] S. Lloyd, Science **321**, 1463 (2008).

[2] S.H. Tan, B.I. Erkmen, V. Giovannetti, S. Guha, S. Lloyd,

L. Maccone, S. Pirandola, and J.H. Shapiro, Phys. Rev. Lett. **101**, 253601 (2008).

[3] K.M.R. Audenaert, J. Calsamiglia, R. Munoz-Tapia, E. Bagan, L. Masanes, A. Acin, and F. Verstraete, Phys. Rev. Lett. **98**, 160501 (2007).

[4] J. Calsamiglia, R. Munoz-Tapia, L. Masanes, A. Acin, and E. Bagan, Phys. Rev. A **77**, 032311 (2008).

[5] S. Pirandola and S. Lloyd, Phys. Rev. A **78**, 012331 (2008).

[6] R. Nair and M. Gu, Optica **7**, 771 (2020).

[7] M. Bradshaw, L.O. Conlon, S. Tserkis, M. Gu, P.K. Lam, and S.M. Assad, Phys. Rev. A **103**, 062413 (2021).

[8] E.D. Lopaeva, I. Ruo Berchera, I.P. Degiovanni, S. Olivares, G. Brida, and M. Genovese, Phys. Rev. Lett. **110**, 153603 (2013).

[9] D.G. England, B. Balaji, and B.J. Sussman, Phys. Rev. A **99**, 023828 (2019).

[10] Y. Zhang, D. England, A. Nomerotski, P. Svihra, S. Ferrante, P. Hockett, and B. Sussman, Phys. Rev. A **101**, 053808 (2020).

[11] S.-Y. Lee, Y.S. Ihn, and Z. Kim, Phys. Rev. A **103**, 012411 (2021).

[12] C. Noh, C. Lee, and S.-Y. Lee, J. Opt. Soc. Am. B **39**, 1316 (2022).

[13] S.-Y. Lee, Y. Jo, T. Jeong, J. Kim, D.H. Kim, D. Kim, D.Y. Kim, Y.S. Ihn, and Z. Kim, Phys. Rev. A **105**, 042412 (2022).

[14] C.W. Sandbo Chang, A. M. Vadiraj, J. Bourassa, B. Balaji, and C.M. Wilson, Appl. Phys. Lett. **114**, 112601 (2019).

[15] D. Luong, C. W. S. Chang, A. M. Vadiraj, A. Damini, C. M. Wilson, B. Balaji, IEEE Trans. Aero. Electron. Syst. **56**, 2041 (2020).

[16] J.N. Blakely, Quantum Rep. **2**, 400 (2020).

[17] Y. Jo, S. Lee, Y.S. Ihn, Z. Kim, and S.-Y. Lee, Phys. Rev. Research **3**, 013006 (2021).

[18] G. Spedalieri and S. Pirandola, Phys. Rev. Research **3**, L042039 (2021).

[19] S. Guha and B.I. Erkmen, Phys. Rev. A **80**, 052310 (2009).

[20] Z. Zhang, S. Mouradian, F.N.C. Wong, and J.H. Shapiro, Phys. Rev. Lett. **114**, 110506 (2015).

[21] S. Barzanjeh, S. Pirandola, D. Vitali, and J.M. Fink, Sci. Adv. **6**, eabb0451 (2020).

[22] Q. Zhuang, Z. Zhang, and J.H. Shapiro, Phys. Rev. Lett. **118**, 040801 (2017).

[23] H. Yang, W. Roga, J.D. Pritchard, and J. Jeffers, Opt. Express **29**, 8199 (2021).

[24] J.H. Shapiro and S. Lloyd, New J. Phys. **11**, 063045 (2009).

[25] M.G.A. Paris, Int. J. Quantum Inf. **7**, 125 (2009).

[26] M. Sanz, U. Las Heras, J.J. García-Ripoll, E. Solano, and R. Di Candia, Phys. Rev. Lett. **118**, 070803 (2017).

[27] See Supplemental Material.

SUPPLEMENTAL MATERIAL

Bargmann representation.—

The Bargmann representation of a state is a compact method to encode the number basis matrix elements in a single function [1]. For example, the Bargmann representation of a one-mode state ρ is a function $K(z, w^*)$ in two variables z, w^* , and the matrix element $\langle n|\rho|m\rangle$ is given as $\sqrt{n!m!} \times (\text{coeff. of } z^n w^{*m})$. Hence by computing the Bargmann representation of the returned states, we have access to all number state probabilities.

The reflected output state when using a displaced squeezed state has Bargmann representation

$$K_{\text{DS}}(z, w^*) = \frac{1}{\sqrt{L}} \exp \left[\frac{1}{2L} \left\{ \frac{1}{2} (A_1^2 - A_2^2 - 1) z w^* - A_2 (e^{i\varphi} z^2 + e^{-i\varphi} w^{*2}) + \sqrt{\kappa} (\alpha (A_1 + 1) + \alpha^* e^{i\varphi} A_2) z + \sqrt{\kappa} (\alpha^* (A_1 + 1) + \alpha e^{-i\varphi} A_2) w^* - \kappa |\alpha|^2 (A_1 + 1 + A_2 \cos(2\phi - \varphi)) \right\} \right], \quad (11)$$

where $A_1 = 1 + 2N_B + 2\kappa N_{sq}$, $A_2 = 2\kappa \sqrt{N_{sq}(N_{sq} + 1)}$, $N_{sq} = \sinh^2 r$, and $L = (N_B + 1)^2 + \kappa N_{sq}(2 + 2N_B - \kappa)$.

The reflected output state when using a TMSV state has Bargmann representation

$$K_{\text{TMSV}}(z_1, z_2, w_1^*, w_2^*) = \frac{1}{E} \exp \left[\frac{2(N_S + 1)(B - 1) - C^2}{4E} z_1 w_1^* + \frac{2N_S(B + 1) - C^2}{4E} z_2 w_2^* + \frac{C}{2E} (z_1 z_2 + w_1^* w_2^*) \right], \quad (12)$$

where $B = 1 + 2\kappa N_S + 2N_B$, $C = 2\sqrt{\kappa N_S(N_S + 1)}$, and $E = (N_B + 1)(N_S + 1)$.

The reflected output state when using a CCT state has Bargmann representation

$$K_{\text{CCT}}(z_1, z_2, w_1^*, w_2^*) = \frac{1}{F} \exp \left[\frac{2(N_I + 1)(B - 1) - D^2}{4F} z_1 w_1^* + \frac{2N_I(B + 1) - D^2}{4F} z_2 w_2^* + \frac{D}{2F} (z_1 w_2^* + w_1^* z_2) \right], \quad (13)$$

where $D = 2\sqrt{\kappa N_I N_I}$ and $F = (N_B + 1)(N_I + 1) + \kappa N_S$.

* suyong2@add.re.kr

† kiow639@add.re.kr

[1] B. C. Hall, Contemporary Mathematics, **260**, 1-59 (2000).